ELSEVIER

Contents lists available at ScienceDirect

Journal of Organometallic Chemistry

journal homepage: www.elsevier.com/locate/jorganchem





Facile synthesis of Copper(I) formamidinates and their photoluminescence properties[#]

Ameen Jowhar Eradiparampath ^a, Zhifang Guo ^a, Glen B. Deacon ^b, Vanitha R. Naina ^c, Julia Feye ^c, Peter W. Roesky ^{c,d}, Peter C. Junk ^{a,*} ^o

- ^a College of Science & Engineering, James Cook University, Townsville, Queensland 4811, Australia
- ^b School of Chemistry, Monash University, Clayton, Victoria, 3800, Australia
- ^c Institute of Inorganic Chemistry, Karlsruhe Institute of Technology, Kaiserstr.12, 76131 Karlsruhe, Germany
- ^d Institute of Nanotechology, Karlsruhe Institute of Technology, Kaiserstr. 12, 76131 Karlsruhe, Germany

ARTICLE INFO

Keywords: Copper(i) Formamidinates Luminescence Structures Synthesis

ABSTRACT

As a part of investigating the reaction of group 11 metal oxides with proligands, a series of luminescent dinuclear Cu(I) formamidinates, $[Cu_2(DippForm)_2]$ (1) (DippForm = N, N'-bis(2,6-diisopropylphenyl)formamidinate), $[Cu_2(EtForm)_2py]$ (2) (EtForm = N, N'-bis(2,6-diiethylphenyl)formamidinate, $[Cu_2(XylForm)_2py]\cdot py)$ (3) (XylForm = N, N'-bis(2,6-diiethylphenyl)formamidinate), $[Cu_2(MesForm)_2py]$ (4) (MesForm = N, N'-bis(2,4,6-trimethylphenyl)formamidinate), $[Cu_2(o-TolForm)_2py]$ (5) (o-TolForm = N, N'-bis(2-trifluoromethylphenyl)formamidinate), $[Cu_2(DFForm)_2(py)_2]$ (7) (DFForm = N, N'-bis(2,6-difluorophenyl)formamidinate), were synthesized by the direct reaction of cuprous oxide with the corresponding formamidine in pyridine. One of the metal centres was coordinated by pyridine in complexes 2-5 and each metal centre was coordinated by solvent molecules in complex 7. The luminescent bimetallic complexes were investigated for their photophysical properties in their solid state. Solid state measurements of the complexes at ambient temperature and at low temperature show phosphorescence emission.

1. Introduction

Coinage metal complexes are known to show special properties compared to other d-block metal analogues owing to their metallophilic interactions [1–4]. Bimetallic metal complexes with interatomic distance less than twice the van der Waals radii of copper, silver and gold show this type of interaction [5,6]. Metallophilic bonding of the coinage metals involves d_{z^2} -d $_{z^2}$ orbital interaction [7]. Multinuclear gold complexes have been studied extensively compared to the silver and copper complexes [8–16]. The tunable synthesis to form gold complexes with intra and intermolecular interactions between Au^+ ions is associated with the formation of low coordination number configurations of polynuclear complexes as well as the aggregation of mononuclear units in crystals [17–20]. The exploration of argentophilic interactions is more limited due to the lower tendency of Ag^+ ions to form linear two coordinate systems [21]. The aurophilic and argentophilic interactions are due to the relativistic effect whereas the reasons behind

cuprophilicity are still debated [22–25]. Multimetallic copper complexes with intra and intermolecular interactions are becoming popular due to their various applications. The cuprophilic interaction is exploited in photoluminescence, which eventually leads to the fabrication of optoelectronic devices, sensors and artificial photosynthesis materials [26–28]. The short Cu-Cu distance is also proposed to have an effect on the superconductivity of Cu₂O based systems [29]. This feature has been employed for developing DNA based copper nanowires for electronic conductivity applications [30]. A significant functional application of the Cu-Cu bond is found in the metalloprotein Cytochrome C oxidase in which its Cu_A centres contain mixed valent Cu atoms, but is not a d^{10} - d^{10} system [31]

Amidinates (RNC(R')NR) are one of the widely explored donor ligands in inorganic chemistry [32–37]. By changing the substituents on the N-C-N backbone, it is possible to fine-tune the electronic and steric properties of the ligand and subsequently achieve metal complexes for specific applications [38]. Metal amidinate complexes have been used in

[#] This paper is dedicated to Prof. Dr Frank Edelmann on the occasion of his 70th birthday and for his outstanding contributions to chemistry thorughout his illustrious career.

^{*} Corresponding author.

polymerizations, [39] hydrogenation, [40] hydroamination, [41] hydrosilylation [42] and CO₂ fixation reactions [43]. Some of the metal amidinate complexes have also found use as precursors for Atomic Layer Deposition (ALD) of thin films [34,44].

Amidinate complexes of group 11 metals were reported decades ago [45]. They have been used to make bimetallic complexes with short M-M distances thereby illustrating the metallophilic character of the complexes [46]. The formation of low coordinate bridged complexes has opened the opportunity to study the metallophilicity [47,48].

There have been many attempts to synthesise copper formamidinates using CuCl and [Cu(NCMe) $_4$][PF $_6$] in metathesis reactions [49,50]. There are no reports of Cu $_2$ O being used for the synthesize of copper formamidinates, whereas it has been used for the synthesis of copper pyrazolate complexes [51–55]. The concomitant Ag $_2$ O has been used for the synthesis of the silver formamidinates and pyrazolates [56]. This work is focused on a convenient synthesis of bimetallic copper(I) formamidinate complexes with different alkyl substituents and their influence on photoluminescence (PL) behaviour at room temperature and at low temperatures.

2. Result and discussion

2.1. Synthesis and characterisation

The direct reaction of Cu₂O and a formamidine in pyridine for a week at room temperature resulted in the formation of bimetallic copper(I) formamidinates [Cu₂(DippForm)₂] (1) (DippForm = N, N'-bis(2,6-diisopropylphenyl)formamidinate), $[Cu_2(EtForm)_2py]$ (2) (EtForm = N,*N'*-bis(2,6-diethylphenyl)formamidinate, py $\{[Cu_2(XylForm)_2py]\cdot py\}\ (3)\ (XylForm = N, N'-bis(2,6-dimethylphenyl)$ formamidinate), $[Cu_2(MesForm)_2py]$ (4) $(MesForm = N, N'-bis(2,4,6-m)_2py]$ trimethylphenyl)formamidinate), [Cu₂(o-TolForm)₂py] (5) (o-TolForm = N, N'-bis(2-methylphenyl)formamidinate), $[Cu_2(CF_3Form)_2]$ (6) $(CF_3Form = N, N'-bis(2-trifluoromethyphenyl)formamidinate),$ $[Cu_2(DFForm)_2(py)_2]$ (7) (DFForm = N, N'-bis(2,6-difluorophenyl)formamidinate) (Scheme 1). Formamidinates with bulky diisopropylphenyl (Dipp) and trifluoromethylphenyl (CF₃) substituents were isolated pyridine-free. Reactions with EtformH, XylformH, MesformH and o-TolformH formed a bimetallic copper formamidinate with one of the Cu^I ions being coordinated by the solvent molecule. Both the copper centres were coordinated by the solvent molecule in complex 7. Whilst one might attribute the greater Lewis acidity of Cu in 7 to the inductive effect of the fluorine substituents, it is noteworthy that trifluoromethyl substitution has no such effect in 6 where steric factors outweigh electronic properties (see structures). The H2O molecule formed as coproduct in the reaction caused decomposition of the product especially the fluorinated copper formamidinates in solution. Pyridine is found to be the best solvent for these reactions, whereas the reactions in other donor solvents such as CH_3CN and tetrahydrofuran were not proceeding.

The isolated yields of all the complexes were moderate to high. Fluorinated copper formamidinates 6 and 7 are more sensitive to air and moisture compared to other complexes. The complexes were characterised by NMR, IR and elemental analysis. ¹H, ¹³C and IR data of **1** are in good agreement with the reported information [50]. Because of the extreme reactivity of the compounds to traces of oxygen, samples for microanalysis were crystals removed from beneath the pyridine mother liquor. As a result, C, H, N analyses for compounds showed the presence of extra pyridine (0.5–1py/complex) which provided protection against oxidation. Complex 1 was analysed as a hydrate and the IR shows a very weak band at 3200 cm⁻¹ to support this. (It is weaker than aromatic ν (CH) as there are numerous aromatic CH bonds but only two OH.) Complex 2 was analysed for loss of py of crystallization. For ¹H NMR measurements, dried bulk crystals were used. Proton decoupled ¹⁹F NMR spectra of 6 and 7 show a single peak at -58.55 ppm and -122.89ppm attributable to CF₃ and aromatic fluorine substituents respectively.

2.2. Molecular structures

Single crystals of all the molecules were grown from saturated solutions in pyridine. The single crystal data of ${\bf 1}$ are in good agreement with those reported by Lane et al. [50]. All complexes are dinuclear with the formamidinates bridging the Cu-Cu vector in a transoid relationship (Figs. 1 and 2). The molecular structures in the solid state of 1 and 6 are centrosymmetric without any py molecule coordinated. In 2-5, a pyridine is coordinated to one Cu atom, whilst 3 has one pyridine of crystallization indicating there is insufficient Lewis acidity at the uncomplexed Cu atom for this to ligate. The N1-Cu1-N3 bond angles are between 176-178° and the N2-Cu2-N4 bond angles are between 158-160° owing to the coordinated py. In the complex 7, and uniquely for the present products, py is coordinated to both Cu atoms. The N1*-Cu1-N2 bond angle is 165.01(5)° and the N3-Cu1-Cu1* bond angle is 151.45(4)°, deviating considerably from linear and distorting the stereochemical array. Complexes 6 and 7 have centrosymmetric structures. The pyridine coordinated metal atom has near square planar stereochemistry whereas the pyridine-free copper atoms have a T-shape coordination array. The lack of pyridine coordination in 1 and 6 can be attributed to the bulky iPr and CF3 groups blocking the approach of py to the Cu atoms. The single CF3 group is orientated towards the Cu atom, when it could be rotated away. There are weak Cu-F interactions in that

2. R = R' = H; R'' = H; n = M = 0 5. R = Me; R = R'' = H; n = 1, m = 0 6. $R = CF_3; R' = R'' = H; n = m = 0$

3. R = R' = Me; R" = H; n = 1, m = 0 7. R = R' = F; R" = H; n = m = 1

4. R = R' = R" = Me; n = 1, m = 0

Scheme 1. Synthesis of copper(I) formamidinates.

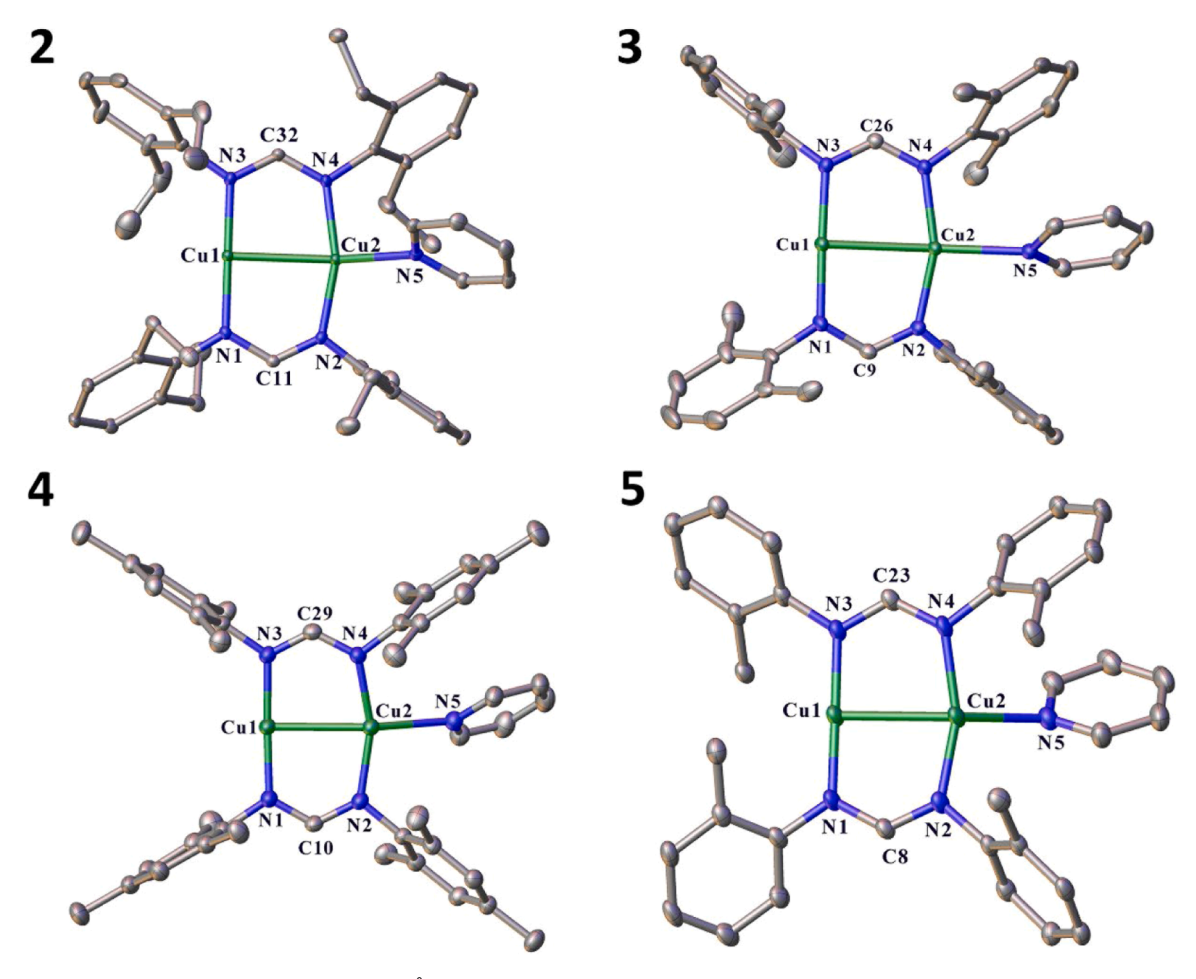


Fig. 1. Molecular structure of 2–5. Selected bond lengths (Å) and angles (°): 2 Cu1-Cu2 2.6158(7), Cu1-N1 1.866(3), Cu1-N3 1.871(3), Cu2-N2 1.923(3), Cu2-N4 1.942(3), Cu2-N5 2.224(3), N1-Cu1-N3 178.19, N2-Cu2-N4 159.63(12), Cu1-Cu2-N5 150.36(7), N1-Cu1-Cu2 89.78(8), N3-Cu1-Cu2 90.07(9), N2-Cu2-Cu1 88.48(5), N4-Cu2-Cu1 89.84(4), N2-Cu2-N5 102.36(11), N4-Cu2-N5 98.00(11); 3 Cu1-Cu2 2.6720(8), Cu1-N1 1.8746(11), Cu1-N3 1.8724(11), Cu2-N2 1.9234(11), Cu2-N4 1.9307(11), Cu2-N5 2.2504(12), N1-Cu1-N3 176.44(4), N2-Cu2-N4 159.72(4), Cu1-Cu2-N5 172.34(3), N1-Cu1-Cu2 89.18(4), N3-Cu1-Cu2 88.93(4), N2-Cu2-Cu1 80.45(4), N4-Cu2-Cu1 81.10(4), N2-Cu2-N5 99.95(5), N4-Cu2-N5 99.47(5); 4 Cu1-Cu2 2.6613(5), Cu1-N1 1.8579(14), Cu1-N3 1.8620(14), Cu2-N2 1.9321(14), Cu2-N4 1.9308(14), Cu2-N5 2.2732(15), N1-Cu1-N3 176.69(6), N2-Cu2-N4 160.43(6), Cu1-Cu2-N5 158.27(4), N1-Cu1-Cu2 88.48(5), N3-Cu1-Cu2 89.84(4), N2-Cu2-Cu1 80.21(4), N4-Cu2-Cu1 81.75(4), N2-Cu2-N5 99.68(6), N4-Cu2-N5 99.89(6); 5 Cu1-Cu2 2.6215(8), Cu1-N1 1.866(4), Cu1-N3 1.868(4), Cu2-N2 1.945 (4), Cu2-N4 1.959(4), Cu2-N5 2.252(4), N1-Cu1-N3 178.24(17), N2-Cu2-N4 158.64(16), Cu1-Cu2-N5 147.12(11), N1-Cu1-Cu2 90.59(11), N3-Cu1-Cu2 89.75(11), N2-Cu2-Cu1 81.17(11), N4-Cu2-Cu1 81.49(10), N2-Cu2-N5 105.28(15), N4-Cu2-N5 96.05(15).

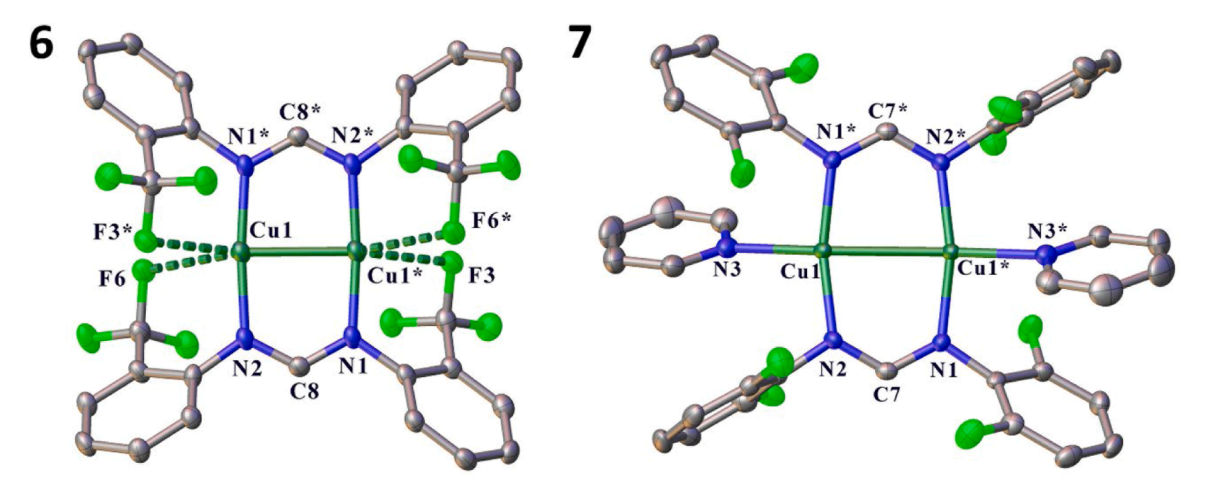


Fig. 2. Molecular structure of 6 and 7. Selected bond lengths (Å) and angles (°): 6 Cu1-Cu1* 2.5046(13), Cu1-N1* 1.871(4), Cu1-N2 1.883(4), Cu1-F3 2.6621(7), Cu1-F6* 2.6749(9), N1*-Cu1-N2 174.60(18), N1*-Cu1-Cu1* 87.05(13), N2-Cu1-Cu1* 87.55(13); 7 Cu1-Cu1* 2.7133(6), Cu1-N1* 1.9294(15), Cu1-N2 1.9183(14), Cu1-N3 2.2644(13), N1*-Cu1-N2 165.01(5), N3-Cu1-Cu1* 151.45(4), N1*-Cu1-Cu1* 83.01(4), N2-Cu1-Cu1* 84.54(4), N1*-Cu1-N3 100.58(5), N2-Cu1-N3 94.35(5).

the Cu1-F3 and Cu1-F6* distances in 6 (2.6621(7) Å and 2.6749(9) Å respectively) are less than the sum of the appropriate van der Waals radii [57-59]. However, the fact that 6 has the shortest Cu-Cu bond indicates that there is negligible electron density transfer from F to Cu, as coordination of py increases the Cu-Cu bond length. (Table 1) Thus, with no pyridine the coordinated Cu-Cu is ca. 2.50- 2.55 Å, with one py Cu-Cu is 2.61–2.67 Å and with two py coordinated, the distance is 2.7133(6) Å. The closest related structures are four copper complexes of chelating μ -1,5-bis(4-substituted phenyl)penta-azadienide ligands each with two pyridines also bound as in 7 [60]. The difference in that there is an N-N-N backbone instead of the N-CH-N array of 1-7. In these reported structures the Cu-N(py) bond lengths are shorter than in 7 by ca. 0.2 Å, and yet the Cu-Cu bond distances are 0.13-0.15 Å shorter than in 7. On the other hand, in compensation, the framework Cu-N bonds average ca. 0.05 Å shorter than those of the reported compounds [60]. Other bonds and angles in 1 and 6 are nearly equivalent.

2.3. Photoluminescence (PL)

The copper(I) formamidinate complexes 1-7, were investigated for their photophysical properties in the solid state. The PL spectra of the complexes at 77 K and room temperature are in Figs. 3 and 4, respectively. The PL data of the complexes in the solid state at 77 K and 295 K are summarized in Table 2. Complex 1, with the disopropyl substituents at the o-position, shows a weak emission with λ_{max} at 460 nm and 415 nm at 77 K and room temperature, respectively (Figure S25). The lifetimes of the excited states could not be determined, since the values are below the detection limit of the detector. Complex 2, with the ethyl substituents, exhibits an emission maximum at 425 nm, which decays biexponentially, with an average lifetime of 422 µs. At room temperature, the complex shows two bands in the PL spectrum: a minor band at 415 nm and a major band at 560 nm. As expected, with increasing temperature, the excited states now decay rapidly with a lifetime of 10 μs. At 77 K, complex 3, with methyl substituents at the o-position, shows an emission band with λ_{max} at 583 nm, which is red-shifted compared to complex 2. The excited state of the complex 3 has a comparatively shorter lifetime (22 μ s) than the complex **2** ($\tau_{avg} = 422 \,\mu$ s). The PL bands of complexes 1-3 do not exhibit a clear trend when the bulkiness of the substituents at the o-position of the complex is varied. However, a clear dependence of the quantum yield on the substituents of the formamidinate ligand is observed among these series of complexes. On decreasing the bulkiness of the alkyl groups, the quantum yield is increased from 2 % (for complex 1) to 37 % (for complex 3). Additionally, the introduction of a methyl group at the p-position of the phenyl ring (complex 4) caused a blue shift in the emission to $\lambda_{max} = 562$ nm at 77 K, compared to complex 3 ($\lambda_{max} = 583$ nm). This complex also shows a hypsochromic shift in the PL band as the temperature increases. The quantum efficiency of complex 4 was measured to be over 90 %, a significant increase compared to complex 3. The molecular packing of complex 3 reveals the presence of an additional pyridine molecule at a distance of 3.47 Å from the copper(I) cation, which is absent in complex 4. We tentatively attribute the lower quantum efficiency of complex 3 (compared to complex 4) to the presence of this non-coordinating pyridine molecule near Cu(I), as it may contribute to enhanced nonradiative decay channels.

Table 1
Cu-Cu bond distances in complexes 1–7.

Complex	Cu-Cu bond length (Å)
1	2.5423(10)
2	2.6158(7)
3	2.6720(8)
4	2.6613(5)
5	2.6215(8)
6	2.5046(13)
7	2.7133(6)

Complex 5, with only one methyl group at the o-position, is non-emissive both at 77 K and room temperature. When the methyl group replaced with the –CF3 group, complex 6 becomes emissive, but only at 77 K with $\lambda_{max}=472$ nm (Fig. 3), which can be attributed to the electronics of the –CF3 group. The lifetime of the excited state is determined to be biexponential, with an average lifetime of 745 μ s ($\tau_{avg}=745$ μ s).

Complex 7, which has fluorine groups at the o-position, is again emissive both at room temperature and 77 K. The complex emits at 540 nm with a quantum efficiency of 14 %. The complex is also phosphorescent like other emissive compounds in this study. These results clearly suggest that the shielding of Cu^I centres by o-substitution of the phenyl ring is crucial to avoid non-radiative decay, which is well known for mononuclear heteroleptic Cu^I complexes [61].

The PL spectra of the complexes were also investigated in pyridine at room temperature for all the complexes (Figure S26). Complexes 1,2 and 6 show emission peaks at 425 nm, 460 nm and 450 nm, respectively. Whereas the complexes 3-5 and 7 show emission peaks at 470 nm. The lifetimes of the complexes in solution state were too low to be measured by our detector.

3. Conclusions

A range of copper formamidinates was synthesized by a convenient direct reaction between cuprous oxide and formamidines. The complexes were characterized by multinuclear NMR, IR and luminescence spectroscopy. The structures of all the complexes were determined by X-ray crystallography. The complexes are bimetallic with solvent coordination except when formamidines with very bulky alkyl derivatives are used (1, 6). Complexes 2–5 show different coordination arrangements on each Cu ion. The Cu-Cu bond lengths of all the complexes were within the range of cuprophilic interactions. The substituents at the *o*- and *p*-positions have a significant influence on the photoluminescence properties. Shielding of the Cu^I centres by alkyl substitution at *o*-position is found to be crucial for the complexes to be emissive at room temperature.

4. Experimental section

4.1. General

The synthesis of the copper compounds was conducted with protection of the reaction mixture from air and moisture under an inert atmosphere (N2) using glove box and standard schlenk techniques. Cuprous oxide (Cu2O) 97 % was purchased from Sigma Aldrich. All formamidine ligands were synthesized according to the literature procedure [62]. Pyridine was distilled from calcium hydride, degassed, and stored over dried 4 Å molecular sieves. C₆D₆ was predried with 4 Å molecular sieves. IR spectra were recorded as Nujol mulls between NaCl plates using an ATR-IR instrument within the range 4000–500 cm⁻¹. ¹H NMR, ¹³C NMR and proton decoupled ¹⁹F NMR spectra were recorded with a Bruker 400 MHz instrument. Chemical shifts were referenced to the residual resonances of the deuterated solvents ($^{1}\mathrm{H}$ and $^{13}\mathrm{C}$). Microanalyses were determined by the Elemental Analysis Service, London Metropolitan University, and all the samples of crystals which were directly removed from under pyridine were sealed in tubes under nitrogen. Metal analysis of the complex 5 was done by EDTA titration with the solid product in pyridine and ammonia solution with fast sulphone black F indicator [63]. Melting points were determined in sealed glass capillaries under nitrogen and are uncalibrated. Crystals were immersed in crystallography oil and were measured on the MX1 beamlines at the Australian Synchrotron. CCDC 2406770-2406775 for compounds 2-7, contain the supplementary crystallographic data for this paper. These data can be obtained free of charge from The Cambridge Crystallographic Data Centre www.ccdc.cam.ac.uk/data request/cif.

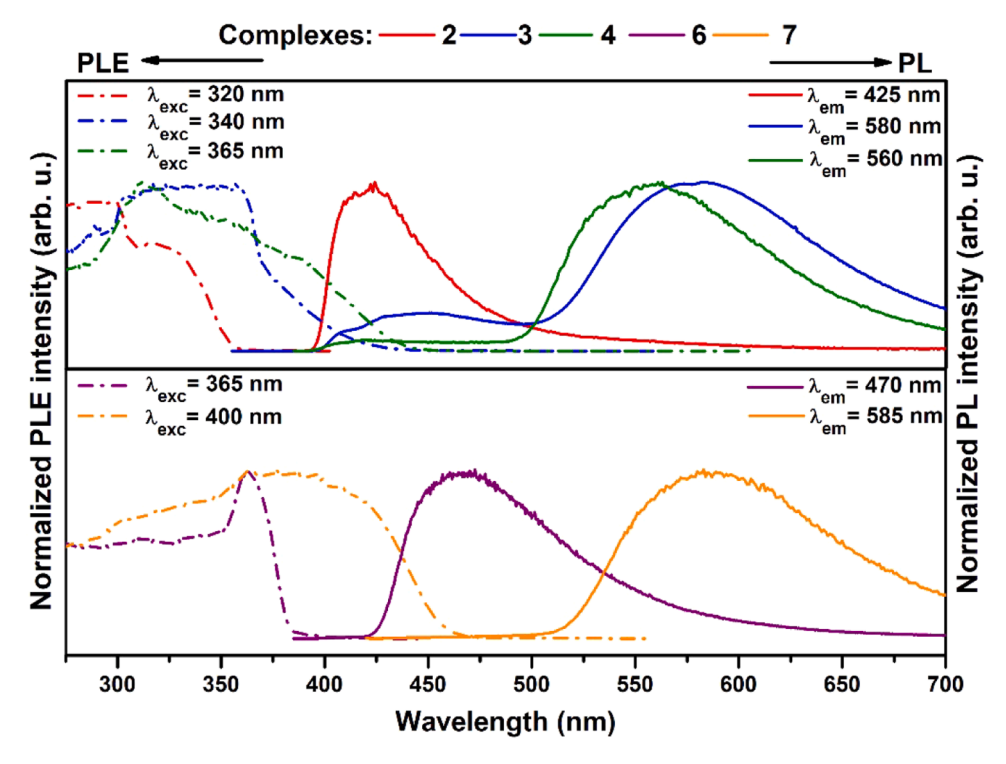


Fig. 3. Normalized photoluminescence excitation (PLE) and emission (PL) spectra of solid complexes at 77 K. PLE and PL spectra were recorded at the depicted wavelengths (λ_{ex} and λ_{em}).

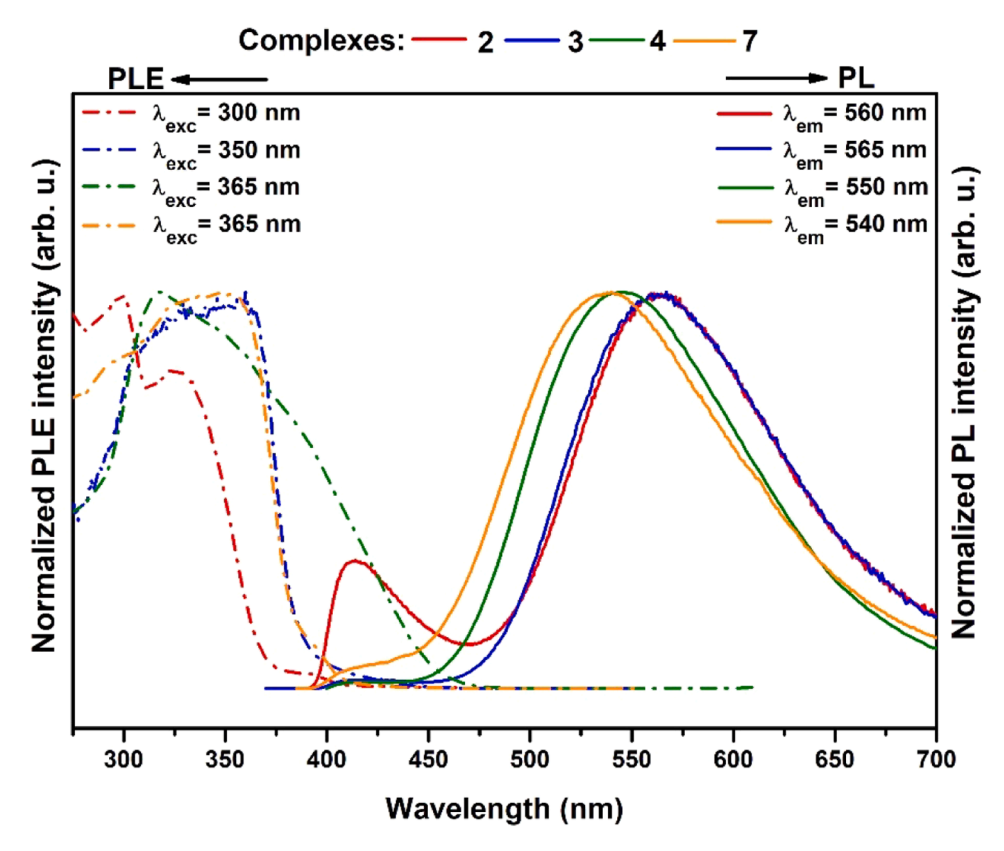


Fig. 4. Normalized photoluminescence excitation (PLE) and emission (PL) spectra of complexes in solid state at room temperature. PLE and PL spectra were recorded at the depicted wavelengths (λ_{ex} and λ_{em}).

Table 2 Photophysical properties of the complexes **1–7** in the solid state.

Complex	Lifetimes of the excited states		λ_{max} (nm)		QY (%)
	rt (μs)	77 K (μs)	rt	77 K	
1	n.d ^a	n.d ^a	415	460	2
2	10	422 ^b	560	425	8
3	13	22	565	583	37
4	15	20	550	562	>90
6	n.d ^c	745 ^b	n.d ^c	472	No emission
7	14(540)	22	540	585	14

- ^a The lifetimes are below the detection limit of our detector.
- b average lifetimes of biexponential decay.
- c complex is non-emissive.

4.2. Synthesis of Cu(I) complexes

 Cu_2O (0.50 mmol) was stirred with the formamidine (1.0 mmol, DippFormH, EtFormH, MesFormH, XylFormH, o-TolFormH, CF $_3$ FormH and DFFormH) in pyridine solvent at room temperature for 7 days. After filtration the solution was concentrated to grow crystals except for the reactions with DFFormH and CF $_3$ FormH. Fresh pyridine was used to grow crystals for $[Cu_2(CF_3Form)_2]$ and $[Cu_2(DFForm)_2(py)_2]$ due to the decomposition of the copper complex by the water molecules formed as co-product. The samples for microanalyses were directly taken from the mother liquor, which caused the extra pyridine solvent in the analysis results (compounds 3, 4, 6 and 7). The samples for NMR were totally dried under vacuum at room temperature except for 7. Crystals of 7 for NMR were directly taken from the mother liquor.

4.2.1. $[Cu_2(DippForm)_2]$ (1)

Colourless crystals (0.190 g, 0.225 mmol, 45 %, m.p. 310–312 °C) were obtained after concentration under vacuum. IR (Nujol) 3200vw, 1663s, 1595w, 1559w, 1253v, 1204m, 1183m, 1160w, 1098s, 1058m, 1002w, 934s, 800s, 776m, 757s cm⁻¹. ¹H NMR (400 MHz, 25 °C, C₆D₆, ppm): δ 7.28(s, 2H, NCHN), 7.18 (m, 12H, Ph), 3.90(m, 8H, CH), 1.37 (m, 48H, Me) ppm. ¹³C NMR (C₆D₆, 100 MHz): δ 165.58 (NCHN), 144.90 (Ph), 137.71 (Ph), 122.58 (Ph), 122.28 (Ph), 27.15(CH), 22.65 (Me) ppm. Elemental Anal. Calcd for C₅₀H₇₀Cu₂N₄ (M = 854.18) calculated C, 70.30, H 8.26, N 6.56; C₅₀H₇₂Cu₂N₄O (872.22, absorbed molecule of water) calculated: C 68.85, H 8.32, N 6.42. found: C 69.04, H 8.43, C 6.36. 1 crystallized in the monoclinic space group C2/c, a 46.510(9) Å, b 10.389(2) Å, c 21.363(4) Å, β 115.52(3)°, V 9315(4) Å which is similar to the results reported in 2014 [50], monoclinic a 46.536(4) Å, b 10.3918(9) Å, c 21.3697(18) Å, β 115.5950(10)°, V 9320.1(14) Å 3.

4.2.2. $[Cu_2(EtForm)_2py]$ (2)

Colourless crystals (0.198 g, 0.24 mmol, 48 %, m.p. 260–262 °C) were obtained after concentration under vacuum. IR (Nujol) 1561w, 1188w, 1103m, 1076w, 1000m, 870s, 800s, 755m, 728m cm⁻¹. ¹H NMR (400 MHz, 25 °C, C_6D_6 , ppm): Before drying: δ 8.53 (s, 2H, NCHN), 7.02 (s, 1H, p-H(py)), 6.92 (m, 12H, Ph), 6.81 (m, 2H, o-H(py)), 6.66 (m, 2H, m-H(py)) 2.86 (m, 16H, -CH₂), 1.24 (t, 24H, Me) ppm. [Cu₂(Et-Form)₂py] after drying; ¹H NMR (400 MHz, 25 °C, C_6D_6 , ppm, loss of the coordinated pyridine): δ 6.95 (m, 12H, Ph), 6.81(s, 2H, NCHN), 2.77 (m, 16H, -CH₂), 1.24 (t, 24H, Me) ppm. ¹³C NMR (C_6D_6 , 100 MHz): δ 169.58 (NCHN), 150.03 (Ph), 145.59 (Ph), 138.76 (Ph), 134.85 (py), 126.57 (Ph), 124.79 (py), 123.17 (py), 25.32 (-CH₂), 14.50 (Me) ppm. Elemental Anal. Calcd for $C_{47}H_{59}Cu_2N_5$ (M = 821.07) calculated C 68.75, H 7.24, N 8.53; $C_{42}H_{54}Cu_2N_4$ (M = 741.99 coordinated pyridine lost) calculated: C 67.99, H 7.34, N 7.55. found: C 68.42, H 7.48, N 7.58.

4.2.3. { $[Cu_2(XylForm)_2py] \cdot py$ } (3)

Yellow crystals (0.157 g, 0.20 mmol, 40 %, m.p. 308-310 °C) were obtained after concentration under vacuum. IR (Nujol) 2725m, 1598w, 1565m, 1252w, 1221w, 1196m, 1161w, 1093m, 1029s, 1004w, 979w,

937w, 916w, 942w, 766m, 756m, 731w, 701m cm $^{-1}$. 1 H NMR (400 MHz, 25 $^{\circ}$ C, C₆D₆, ppm; loss of py of crystallisation): δ 8.52 (s, 2H, NCHN), 6.97 (m, 2H, o-H(py)), 6.85 (m, 12H, Ph), 6.66 (m, 2H, m-H(py)), 6.58 (m, 1H, p-H(py)), 2.27 (s, 24H, Me). 13 C NMR (C₆D₆, 100 MHz, ppm): δ 170.13(NCHN), 146.77(Ph), 132.61(Ph), 128.31(Ph), 124.17(Ph), 19.05(Me). Elemental Anal. Calcd for C₄₄H₄₈Cu₂N₆ (M = 819.69) C 67.07, H 6.14, N 10.67; C₄₉H₅₃Cu₂N₇ (M = 867.08 added 1 mol of pyridine) calculated: C 67.87, H 6.16, N 11.31. found: C 68.34, H 6.12, N 11.22.

4.2.4. $[Cu_2(MesForm)_2py]$ (4)

Yellow crystals (0.145 g, 0.19 mmol, 38 %, m.p. 245–247 °C) were obtained after concentration under vacuum. IR (Nujol) 2725w, 1612m, 1574s, 1376vs, 1336m, 1261vw, 1232w, 1211m, 1146w, 1029w, 848m, 800w, 722m, 701m cm $^{-1}$. 1 H NMR (400 MHz, 25 °C, C₆D₆, ppm-loss of py of crystallization): δ 8.53 (s, 2H, NCHN), 6.95 (m, 2H, o-H(py)), 6.73 (m, 2H, m-H(py)), 6.68 (m, 8H, Ph),6.64 (m, 1H, p-H(py)), 2.32 (s, 24H, o-Me), 2.10 (s, 12H, p-Me). 13 C NMR (C₆D₆, 100 MHz, ppm): δ 170.40 (NCHN), 144.56 (Ph), 133.10 (Ph), 132.28 (Ph), 129.09 (Ph), 20.45 (p-Me), 19.19 (o-Me). Elemental Anal. Calcd for C₄₃H₅₁Cu₂N₅ (M = 764.96) C 67.51, H 6.72, N 9.15; C_{45.5}H_{53.5}Cu₂N_{5.5} (M = 804.54 added 0.5 mol of pyridine) calculated: C 67.93, H 6.70, N 9.58. found: C 67.32, H 6.61, N 10.11.

4.2.5. $[Cu_2(o\text{-}TolForm)_2py]$ (5)

Colourless crystals (0.143 g, 0.22 mmol, 44 %, m.p. 210–212 °C) were obtained after concentration under vacuum. IR (Nujol) 1462vs, 1377s, 1260m, 1020w, 797m, 722m cm $^{-1}$. ^{1}H NMR (400 MHz, 25 °C, C₆D₆, ppm) coordinated py lost on drying: δ 7.70 (s, 2H, NCHN), 6.92 (m, 16H, Ph), 2.05 (s, 12H, Me). ^{13}C NMR (C₆D₆, 100 MHz, ppm): δ 146.25 (NCHN), 130.45 (Ph), 126.83 (Ph), 123.00 (Ph), 117.54 (Ph), 17.59 (Me). Cu analysis calculated for $\text{C}_{35}\text{H}_{35}\text{Cu}_2\text{N}_5$ calculated: Cu 19.47. found: Cu 18.93.

4.2.6. [Cu₂(CF₃Form)₂] (6)

Colourless crystals (0.0789 g, 0.10 mmol, 20 %, m.p. 211–213 °C) were obtained after concentration under vacuum. IR (Nujol) 3416w, 1968w, 1932w, 1898w, 1811w, 1649w, 1518w, 1460m, 1376w, 1260w, 1090w, 825w, 757w, 670w cm $^{-1}$. $^{19}\mathrm{F}$ NMR (376 MHz, 25 °C, $\mathrm{C_6D_6}$, ppm) δ –58.55. $^{1}\mathrm{H}$ NMR (400 MHz, 25 °C, $\mathrm{C_6D_6}$, ppm): δ 7.27 (m, 4H, Ph), 7.21(s, 2H, NC(H)N), 6.87 (m, 4H, Ph), 6.75 (m, 4H, Ph), 6.60 (m, 4H, Ph). $^{13}\mathrm{C}$ NMR (C₆D₆, 100 MHz, ppm): δ 168.76 (NCHN), 147.95 (Ph), 146.39 (Ph), 132.41 (Ph), 126.23 (Ph), 123.99 (Ph), 122.81 (Ph), 120.60 (CF₃). Elemental Anal. Calcd for $\mathrm{C_{30}H_{18}Cu_2F_{12}N_4}$ (M = 789.56) C 45.64, H 2.30, N 7.10; $\mathrm{C_{32.5}H_{20.5}Cu_2F_{12}N_{4.5}}$ (M = 829.115 added 0.5 mol of pyridine) calculated: C 47.08, H 2.49, N 7.60. found: C 47.92, H 2.00, N 7.24.

4.2.7. $[Cu_2(DFForm)_2(py)_2]$ (7)

Yellow crystals (38 %, 0.156 g, 0.19 mmol, m.p. 295–297 °C) were obtained after concentration under vacuum. IR (Nujol) 2722w, 1902w, 1831w, 1751w, 1692w, 1664vw, 1620m, 1560w, 1376ws, 1261m, 1226w, 1153w, 1062m, 1006w, 990m, 872w, 842w, 776s, 730m, 718m, 700m, 629w, 611vw, 560w cm⁻¹. ¹⁹F NMR (376 MHz, 25 °C, C_6D_6 , ppm) δ –122.89. ¹H NMR (400 MHz, 25 °C, C_6D_6 , ppm): δ 8.53 (m, 8H, o-H (py)), 7.71 (s, 2H, NCHN), 6.95 (m, 4H, p-H(Ph)), 6.64 (m, 8H, m-H (Ph)), 6.49 (m, 8H, m-H(py)), 6.32 (m, 4H, p-H(py)) ppm, with excess pyridine from the solution. ¹³C NMR (C_6D_6 , 100 MHz, ppm): δ 170.28 (NCHN), 149.07 (Ph), 133.93 (Ph), 122.34 (Ph), 110.58 (Ph). Elemental Anal. Calcd for $C_{36}H_{24}Cu_2F_8N_6$ (M = 819.69) C 52.75, H 2.95 N 10.25; $C_{41}H_{29}Cu_2F_8N_7$ (M = 898.79 added 1 mol of pyridine) calculated: C 54.79, H 3.25, N 10.91. found: C, 54.21, H 3.44, N 10.60.

CRediT authorship contribution statement

Ameen Jowhar Eradiparampath: Writing - review & editing,

Writing – original draft, Methodology, Investigation, Formal analysis, Data curation. Zhifang Guo: Writing – review & editing, Methodology, Investigation, Formal analysis, Data curation. Glen B. Deacon: Writing – review & editing, Supervision, Methodology, Investigation, Funding acquisition, Conceptualization. Vanitha R. Naina: Writing – review & editing, Formal analysis, Data curation. Julia Feye: Formal analysis, Data curation. Peter W. Roesky: Writing – review & editing, Resources, Methodology, Data curation. Peter C. Junk: Writing – review & editing, Supervision, Project administration, Methodology, Investigation, Funding acquisition, Conceptualization.

Declaration of competing interest

The authors declare no conflicts of interest.

Acknowledgement

GBD and PCJ gratefully acknowledge the ARC for funding (DP230100112). Parts of this research were undertaken on the MX1 beamline at the Australian Synchrotron, part of ANSTO [64] VRN and PWR acknowledge the DFG funded GRK 2039 Molecular Architectures for Fluorescent Cell Imaging for the financial support.

Supplementary materials

Supplementary material associated with this article can be found, in the online version, at doi:10.1016/j.jorganchem.2025.123642.

Data availability

Data will be made available on request.

References

- P.K. Mehrotra, R. Hoffmann, Copper(I)-copper(I) interactions. Bonding relationships in d10-d10 systems, Inorg. Chem. 17 (1978) 2187–2189, https://doi. org/10.1021/ic50186a032.
- [2] H.L. Hermann, G. Boche, P. Schwerdtfeger, Metallophilic interactions in closed-shell copper(I) compounds—A theoretical study, Chem. Eur. J. 7 (2001) 5333–5342, https://doi.org/10.1002/1521-3765(20011217)7:24<5333:: AID—CHEM5333>3.0.CO:2-1.
- [3] S. Burguera, A. Bauzá, A. Frontera, A novel approach for estimating the strength of argentophilic and aurophilic interactions using QTAIM parameters, Phys. Chem. Chem. Phys. 26 (2024) 16550–16560, https://doi.org/10.1039/D4CP00410H.
- [4] P. Pyykkö, J. Li, N. Runeberg, Predicted ligand dependence of the Au(I)...Au(I) attraction in (XAuPH3)2, Chem. Phys. Lett. 218 (1994) 133–138, https://doi.org/10.1016/0009-2614(93)E1447-0.
- [5] K.M. Merz Jr., R. Hoffmann, d10-d10 Interactions: multinuclear copper(I) complexes, Inorg. Chem. 27 (1988) 2120–2127, https://doi.org/10.1021/ic00285a022.
- [6] M. Jansen, Homoatomic d10–d10 interactions: their effects on structure and chemical and physical properties, Angew. Chem. Int. Ed. Engl. 26 (1987) 1098–1110, https://doi.org/10.1002/anie.198710981.
- [7] M.B. Brands, J. Nitsch, C.F. Guerra, Relevance of orbital interactions and Pauli repulsion in the metal-Metal bond of coinage metals, Inorg. Chem. 57 (2018) 2603–2608, https://doi.org/10.1021/acs.inorgchem.7b02994.
- [8] V.W.-W. Yam, E.C.-C. Cheng, Molecular gold—Multinuclear gold(I) complexes, Angew. Chem. Int. Ed. 39 (2000) 4240–4242, https://doi.org/10.1002/1521-3773 (20001201)39:23<4240::AID—ANIE4240>3.0.CO;2-D.
- [9] S. Cheng, Z. Chen, Y. Yin, Y. Sun, S. Liu, Progress in mechanochromic luminescence of gold(I) complexes, Chin. Chem. Lett. 32 (2021) 3718–3732, https://doi.org/ 10.1016/j.cclet.2021.05.049.
- [10] D. Weber, M.R. Gagné, Aurophilicity in gold(I) catalysis: for better or worse? in: L. M. Slaughter (Ed.), Homog. Gold Catal Springer International Publishing, Cham, 2015, pp. 167–211, https://doi.org/10.1007/128_2014_585.
- [11] M.C. Gimeno, A. Laguna, Three- and four-coordinate gold(I) complexes, Chem. Rev. 97 (1997) 511–522, https://doi.org/10.1021/cr960361q.
- [12] M. Concepción Gimeno, A. Laguna, Chalcogenide centred gold complexes, Chem. Soc. Rev. 37 (2008) 1952–1966, https://doi.org/10.1039/B708618K.
- [13] H. Schmidbaur, H.G. Raubenheimer, Excimer and exciplex formation in gold(I) complexes preconditioned by aurophilic interactions, Angew. Chem. Int. Ed. 59 (2020) 14748–14771, https://doi.org/10.1002/anie.201916255.
- [14] E.R.T. Tiekink, Supramolecular assembly of molecular gold(I) compounds: an evaluation of the competition and complementarity between aurophilic (Au···Au) and conventional hydrogen bonding interactions, Coord. Chem. Rev. 275 (2014) 130–153, https://doi.org/10.1016/j.ccr.2014.04.029.

- [15] H. Schmidbaur, A. Schier, Aurophilic interactions as a subject of current research: an up-date, Chem. Soc. Rev. 41 (2012) 370–412, https://doi.org/10.1039/ C1CC15182C
- [16] T.P. Seifert, V.R. Naina, T.J. Feuerstein, N.D. Knöfel, P.W. Roesky, Molecular gold strings: aurophilicity, luminescence and structure–property correlations, Nanoscale 12 (2020) 20065–20088, https://doi.org/10.1039/D0NR04748A.
- [17] L.-S. Wang, Covalent gold, Phys. Chem. Chem. Phys. 12 (2010) 8694–8705, https://doi.org/10.1039/C003886E.
- [18] P. Schwerdtfeger, P.D.W. Boyd, A.K. Burrell, W.T. Robinson, M.J. Taylor, Relativistic effects in gold chemistry. 3. Gold(I) complexes, Inorg. Chem. 29 (1990) 3593–3607, https://doi.org/10.1021/ic00343a057.
- [19] P.G. Jones, X-ray structural investigations of gold compounds, Gold. Bull. 19 (1986) 46–57, https://doi.org/10.1007/BF03214643.
- [20] V.R. Naina, A.K. Singh, J.Krämer Shubham, M. Iqbal, P.W. Roesky, Synthesis of luminescent coumarin-substituted phosphinoamide-bridged polynuclear gold(I) metallacycles and reactivity studies, Inorg. Chem. Front. 11 (2024) 6079–6088, https://doi.org/10.1039/D4Q101747A.
- [21] H. Schmidbaur, A. Schier, Argentophilic interactions, Angew. Chem. Int. Ed. 54 (2015) 746–784, https://doi.org/10.1002/anie.201405936.
- [22] P. Pyykkö, N. Runeberg, F. Mendizabal, Theory of the d10-d10 closed-shell attraction: 1. Dimers near equilibrium, Chem. – Eur. J. 3 (1997) 1451–1457, https://doi.org/10.1002/chem.19970030911.
- [23] P. Pyykkö, X.-G. Xiong, J. Li, Aurophilic attractions between a closed-shell molecule and a gold cluster, Faraday Discuss. 152 (2011) 169–178, https://doi. org/10.1039/CIFD00018G
- [24] S. Dinda, A.G. Samuelson, The nature of bond critical points in dinuclear copper(I) complexes, Chem. Eur. J. 18 (2012) 3032–3042, https://doi.org/10.1002/chem.201101219.
- [25] M.A. Carvajal, S. Alvarez, J.J. Novoa, The nature of intermolecular CuI···CuI interactions: a combined theoretical and structural database analysis, Chem. Eur. J. 10 (2004) 2117–2132, https://doi.org/10.1002/chem.200305249.
- [26] E. Cariati, E. Lucenti, C. Botta, U. Giovanella, D. Marinotto, S. Righetto, Cu(I) hybrid inorganic-organic materials with intriguing stimuli responsive and optoelectronic properties, Coord. Chem. Rev. 306 (2016) 566–614, https://doi.org/10.1016/j.ccr.2015.03.004.
- [27] K. Tsuge, Y. Chishina, H. Hashiguchi, Y. Sasaki, M. Kato, S. Ishizaka, N. Kitamura, Luminescent copper(I) complexes with halogenido-bridged dimeric core, Coord. Chem. Rev. 306 (2016) 636–651, https://doi.org/10.1016/j.ccr.2015.03.022.
- [28] V.R. Naina, A.K. Singh, P. Rauthe, S. Lebedkin, M.T. Gamer, M.M. Kappes, A.-N. Unterreiner, P.W. Roesky, Phase-dependent long persistent phosphorescence in coumarin-phosphine-based coinage metal complexes, Chem. – Eur. J. 29 (2023) e202300497. https://doi.org/10.1002/chem.202300497.
- [29] J.M. Zuo, M. Kim, M. O'Keeffe, J.C.H. Spence, Direct observation of d-orbital holes and Cu–Cu bonding in Cu2O, Nature 401 (1999) 49–52, https://doi.org/10.1038/ 43403.
- [30] G. Li, H. Liu, X. Chen, L. Zhang, Y. Bu, Multi-copper-mediated DNA base pairs acting as suitable building blocks for the DNA-based nanowires, J. Phys. Chem. C 115 (2011) 2855–2864, https://doi.org/10.1021/jp107605k.
- [31] K.R. Williams, D.R. Gamelin, L.B. LaCroix, R.P. Houser, W.B. Tolman, T.C. Mulder, S. de Vries, B. Hedman, K.O. Hodgson, E.I. Solomon, Influence of copper—sulfur covalency and copper—copper bonding on valence delocalization and electron transfer in the CuA site of cytochrome c oxidase, J. Am. Chem. Soc. 119 (1997) 613–614, https://doi.org/10.1021/ja963225b.
- [32] F.T. Edelmann, D.M.M. Freckmann, H. Schumann, Synthesis and structural chemistry of non-cyclopentadienyl organolanthanide complexes, Chem. Rev. 102 (2002) 1851–1896, https://doi.org/10.1021/cr010315c.
- [33] F.T. Edelmann, Chapter 3 advances in the coordination chemistry of Amidinate and Guanidinate ligands, in: A.F. Hill, M.J. Fink (Eds.), Adv. Organomet. Chem, Academic Press, 2008, pp. 183–352, https://doi.org/10.1016/S0065-3055(08)
- [34] F.T. Edelmann, Lanthanide amidinates and guanidinates: from laboratory curiosities to efficient homogeneous catalysts and precursors for rare-earth oxide thin films, Chem. Soc. Rev. 38 (2009) 2253–2268, https://doi.org/10.1039/ B800100F
- [35] F.T. Edelmann, Lanthanide amidinates and guanidinates in catalysis and materials science: a continuing success story, Chem. Soc. Rev. 41 (2012) 7657–7672, https://doi.org/10.1039/C2CS35180C.
- [36] F.T. Edelmann, Recent progress in the chemistry of metal amidinates and guanidinates, in: A.F. Hill, M.J. Fink (Eds.), Adv. Organomet. Chem, Academic Press, 2013, pp. 55–374, https://doi.org/10.1016/B978-0-12-407692-1.00002-3
- [37] V.R.Naina Shubham, P.W. Roesky, Luminescent tetranuclear copper(I) and gold(I) heterobimetallic complexes: a phosphine acetylide amidinate orthogonal ligand framework for selective complexation, Chem. Eur. J. 30 (2024) e202401696, https://doi.org/10.1002/chem.202401696.
- [38] J.A.R. Schmidt, J. Arnold, First-row transition metal complexes of sterically-hindered amidinates, J. Chem. Soc. Dalton Trans. (2002) 3454–3461, https://doi.org/10.1039/B202737M.
- [39] W. Li, S.-D. Bai, F. Su, S.-F. Yuan, X.-E. Duan, D.-S. Liu, Zirconium complexes based on an ethylene linked amidinate-amido ligand: synthesis, characterization and ethylene polymerization, New J. Chem. 41 (2017) 661–670, https://doi.org/ 10.1039/C6N.102537D
- [40] L.M. Martínez-Prieto, I. Cano, A. Márquez, E.A. Baquero, S. Tricard, L. Cusinato, I. del Rosal, R. Poteau, Y. Coppel, K. Philippot, B. Chaudret, J. Cámpora, P.W.N. M. van Leeuwen, Zwitterionic amidinates as effective ligands for platinum nanoparticle hydrogenation catalysts, Chem. Sci. 8 (2017) 2931–2941, https://doi.org/10.1039/C6SC05551F.

- [41] T.S. Brunner, P. Benndorf, M.T. Gamer, N. Knöfel, K. Gugau, P.W. Roesky, Enantiopure amidinate complexes of the rare-earth elements, Organometallics. 35 (2016) 3474–3487, https://doi.org/10.1021/acs.organomet.6b00523.
- [42] S. Ge, A. Meetsma, B. Hessen, Highly efficient hydrosilylation of alkenes by organoyttrium catalysts with sterically demanding amidinate and guanidinate ligands, Organometallics. 27 (2008) 3131–3135, https://doi.org/10.1021/ om800033a
- [43] M.P. Coles, R.F. Jordan, Cationic aluminum alkyl complexes incorporating amidinate ligands. Transition-metal-free ethylene polymerization catalysts, J. Am. Chem. Soc. 119 (1997) 8125–8126, https://doi.org/10.1021/ja971815j.
- [44] F.A. Cotton, J.H. Matonic, C.A. Murillo, Synthesis and structural studies of platinum complexes containing monodentate, bridging, and chelating formamidine ligands, Inorg. Chem. 35 (1996) 498–503, https://doi.org/10.1021/ic950741e.
- [45] W. Bradley, I. Wright, 129. Metal derivatives of NN'-diarylamidines, J. Chem. Soc. Resumed (1956) 640–648, https://doi.org/10.1039/JR9560000640.
- [46] A.A. Mohamed, H.E. Abdou, M.D. Irwin, J.M. López-de-Luzuriaga, J.P. Fackler, Gold(I) formamidinate clusters: the structure, luminescence, and electrochemistry of the tetranuclear, base-free [Au4(ArNC(H)NAr)4], J. Clust. Sci. 14 (2003) 253–266, https://doi.org/10.1023/B.JOCL.0000005062.20754.5f.
- [47] J. Barker, M. Kilner, The coordination chemistry of the amidine ligand, Coord. Chem. Rev. 133 (1994) 219–300, https://doi.org/10.1016/0010-8545(94)80059-6
- [48] F. Krätschmer, X. Gui, M.T. Gamer, W. Klopper, P.W. Roesky, Systematic investigation of the influence of electronic substituents on dinuclear gold(I) amidinates: synthesis, characterisation and photoluminescence studies, Dalton. Trans. 51 (2022) 5471–5479, https://doi.org/10.1039/D1DT03795A.
- [49] P.I.V. Vliet, G.V. Koten, K. Vrieze, Complexes of N,N'-substituted formamidines I. Compounds [M(RNC(H)NR')]n (M=CuI, AgI; R=p-TOLYL; R'=ALKYL; n=2,4); and study of the dimer-dimer and dimer-tetramer equilibria in solution, J. Organomet. Chem. 179 (1979) 89–100, https://doi.org/10.1016/S0022-328X(00)87799-2.
- [50] A.C. Lane, M.V. Vollmer, C.H. Laber, D.Y. Melgarejo, G.M. Chiarella, J.P. Jr. Fackler, X. Yang, G.A. Baker, J.R. Walensky, Multinuclear copper(I) and silver (I) amidinate complexes: synthesis, luminescence, and CS2 insertion reactivity, Inorg. Chem. 53 (2014) 11357–11366, https://doi.org/10.1021/ic501694d.
- [51] N. Masciocchi, M. Moret, P. Cairati, A. Sironi, G.A. Ardizzoia, G.La Monica, The multiphase nature of the Cu(pz) and Ag(pz) (Hpz = Pyrazole) systems: selective syntheses and ab-initio X-ray powder diffraction structural characterization of copper(I) and silver(I) pyrazolates, J. Am. Chem. Soc. 116 (1994) 7668–7676, https://doi.org/10.1021/ja00096a025.
- [52] H.V. Rasika Dias, S.A. Polach, Z. Wang, Coinage metal complexes of 3,5-bis(tri-fluoromethyl)pyrazolate ligand: synthesis and characterization of { [3,5-(CF3)2Pz] Cu}3 and { [3,5-(CF3)2Pz]Ag}3, J. Fluor. Chem. 103 (2000) 163–169, https://doi.org/10.1016/S0022-1139(99)00313-9.

- [53] C.V. Hettiarachchi, M.A. Rawashdeh-Omary, D. Korir, J. Kohistani, M. Yousufuddin, H.V.R. Dias, Trinuclear copper(I) and silver(I) adducts of 4chloro-3,5-bis(trifluoromethyl)pyrazolate and 4-bromo-3,5-bis(trifluoromethyl) pyrazolate, Inorg. Chem. 52 (2013) 13576–13583, https://doi.org/10.1021/ ic402080v.
- [54] Z. Guo, J. Luu, V. Blair, G.B. Deacon, P.C. Junk, Replacing mercury: syntheses of lanthanoid pyrazolates from free lanthanoid metals, pentafluorophenylsilver, and pyrazoles, aided by a facile synthesis of polyfluoroarylsilver compounds, Eur. J. Inorg. Chem. 2019 (2019) 1018–1029, https://doi.org/10.1002/ejic.201801481.
- [55] Z. Guo, V.L. Blair, G.B. Deacon, P.C. Junk, Widely contrasting outcomes from the use of tris(pentafluorophenyl)bismuth or pentafluorophenylsilver as oxidants in the reactions of lanthanoid metals with N,N'-diarylformamidines, Dalton. Trans. 49 (2020) 13588–13600, https://doi.org/10.1039/D0DT03044A.
- [56] Z. Guo, N. Wang, V.L. Blair, E.I. Izgorodina, G.B. Deacon, P.C. Junk, Facile synthesis and structures of silver formamidinates and pyrazolates†, Aust. J. Chem. 75 (2022) 558–565, https://doi.org/10.1071/CH21282.
- [57] S.S. Batsanov, Van der Waals radii of elements, Inorg. Mater. 37 (2001) 871–885, https://doi.org/10.1023/A:1011625728803.
- [58] S. Alvarez, A cartography of the van der Waals territories, Dalton. Trans. 42 (2013) 8617–8636, https://doi.org/10.1039/C3DT50599E.
- [59] G.B. Deacon, P.C. Junk, D. Werner, Lanthanoid induced C-F activation of all fluorine atoms of one CF3 group, Eur. J. Inorg. Chem. 2015 (2015) 1484–1489, https://doi.org/10.1002/ejic.201500137.
- [60] R. Schmid, J. Strähle, Synthese und, Struktur von Pentaazadienido-komplexen des ein- und zweiwertigen Kupfers Kristallstrukturen von [Cu(F-C6H4N5C6H4-F) (py)]2, [Cu(Cl-C6H4N5C6H4-Cl)(py)]2 und [Cu(CH3O-C6H4N5C6H4-OCH3) (py)]2, Z. Für Anorg. Allg. Chem. 575 (1989) 187–196, https://doi.org/10.1002/ zaac.19895750122.
- [61] M. Santander-Nelli, D. Cortés-Arriagada, L. Sanhueza, P. Dreyse, Dependence between luminescence properties of Cu(I) complexes and electronic/structural parameters derived from steric effects, New J. Chem. 46 (2022) 10584–10593, https://doi.org/10.1039/D2NJ00407K.
- [62] E.C. Taylor, W.A. Ehrhart, A convenient synthesis of N,N'-disubstituted formamidines and Acetamidines1, J. Org. Chem. 28 (1963) 1108–1112, https:// doi.org/10.1021/jo01039a061.
- [63] J. Basset, R.C. Denney, G.H. Jeffery, J. Mendham. Vogel's Textbook of Quantitative Inorganic Analysis. 4th Edition. Longmann Group Ltd. New York. 1978. p. 319.
- [64] N.P. Cowieson, D. Aragao, M. Clift, D.J. Ericsson, C. Gee, S.J. Harrop, N. Mudie, S. Panjikar, J.R. Price, A. Riboldi-Tunnicliffe, MX1: a bending-magnet crystallography beamline serving both chemical and macromolecular crystallography communities at the Australian Synchrotron, J. Synchrotron Radiat. 22 (2015) 187–190.